

Telocytes as a Novel Structural Component in the Muscle Layers of the Goat Rumen

Yu Liang¹, Siyi Wang¹, Tianci An¹, Imran Tarique¹,
Waseem Ail Vistro¹, Yifei Liu¹, Ziyu Wang², Haiyan Zhang³,
YongHong Shi^{1,4}, Abdul haseeb¹, Noor Samad Gandahi¹,
Adeela Iqba¹, Huan Yang¹, Qiusheng Chen¹, and Ping Yang^{1,2}

Cell Transplantation
2019, Vol. 28(7) 955–966
© The Author(s) 2019
Article reuse guidelines:
sagepub.com/journals-permissions
DOI: 10.1177/0963689719842514
journals.sagepub.com/home/ctj



Abstract

Telocytes (TCs) have been identified as a distinct type of interstitial cells, but have not yet been reported in the gastrointestinal tract (GIT) of ruminants. In this study, we used transmission electron microscopy (TEM) and double-labelling immunofluorescence (IF) (antibodies: CD34, vimentin and PGP9.5) to seek TCs and investigate their potential functions in the muscle layers of the goat rumen. TCs were distributed widely in the myenteric plexus (TC-MYs) between the circular and longitudinal muscle layers, within circular muscle layers (TC-CMs) as well as in longitudinal muscle layers (TC-LMs). Ultrastructurally, TCs displayed small cell bodies with several long prolongations—telopodes—harboring alternate thin segments (podomers) and dilated segments (podoms). The podoms contained mitochondria, rough endoplasmic reticulum, and caveolae. Telopodes frequently established close physical interactions with near telopodes, collagen fibers (CFs), nerve fibers (NFs), smooth muscle cells (SMCs), nerve tracts, and smooth muscle bundles, as well as with blood vessels (BVs). Furthermore, both homo- and heterotypic connections were observed. In addition, telopodes were capable of releasing extracellular vesicles (EVs). IF analyses proved that TCs were reliably labeled as CD34+/vimentin+ cells, displaying spindle- or triangle-shaped bodies with long prolongations, consistent with TEM results. Specifically, podoms were visible as obvious bright spots. These positive cells covered entire muscular layers, surrounding ganglions, intermuscular BVs as well as entire smooth muscle bundles, forming a network. TC-MYs were distributed as clusters in the external ganglion, encompassing the entire ganglion and spreading to the muscle layers where TC-CMs and TC-LMs seemingly surround whole smooth muscle bundles. TC-MYs were also scattered within the interior of the ganglion, surrounding each ganglionic neuron, following the glial cells layer. We speculate that TCs support the muscle layer structure of the goat rumen and facilitate intercellular signaling directly or indirectly via the TC network.

Keywords

Telocyte, telopodes, muscle layers, rumen

Introduction

The telocyte (TC) is a novel type of interstitial cell in the gastrointestinal tract (GIT) of several monogastric animals. According to Popescu, their discoverer, the most significant feature of TCs is the presence of a unique telopode, an extremely long and moniliform of projection displaying an alternation of thin segments (podomers) and dilated segments (podoms)¹. At the ultrastructural level, podoms contain caveolae, mitochondria, and endoplasmic reticulum^{1–3}. TC identification is based on the ultrastructural criteria suggested by Popescu¹. However, in recent years, histological and immunological studies have revealed that the most relevant TC identification criteria rely on CD34, tyrosine

¹ MOE Joint International Research Laboratory of Animal Health and Food Safety, College of Veterinary Medicine, Nanjing Agricultural University, Jiangsu, China

² College of Animal Science & Technology, Nanjing Agricultural University, Jiangsu, China

³ School of Biological Engineering, Wuhu Institute of Technology, Anhui, China

⁴ Shanghai Veterinary Research Institute, Chinese Academy of Agricultural Sciences, China

Submitted: December 22, 2018. Revised: February 25, 2019. Accepted: March 11, 2019.

Corresponding Author:

Ping Yang, Nanjing Agricultural University, Weigang road 1, Nanjing, Jiangsu 210095, China.

Email: yangping@njau.edu.cn



Creative Commons Non Commercial CC BY-NC: This article is distributed under the terms of the Creative Commons Attribution-NonCommercial 4.0 License (<http://www.creativecommons.org/licenses/by-nc/4.0/>) which permits non-commercial use, reproduction and distribution of the work without further permission provided the original work is attributed as specified on the SAGE and Open Access pages (<https://us.sagepub.com/en-us/nam/open-access-at-sage>).

kinase receptor (c-kit) and vimentin, platelet-derived growth factor receptor (PDGFR), Caveolin-1, etc.^{1,2,4-12}. Due to various unknown functional features of TCs, this results in different immunophenotype appearances. TCs may have different immunophenotypes according to their tissue localization. Therefore, immunofluorescence (IF), another accepted method for TCs identification, showed that TCs can express at least two markers among CD34, c-kit and vimentin *in vivo* or *in vitro*^{1,2,5-7,10,11}. TCs frequently established homo- and heterotypic connections with other structures (nerve fibers (NFs), blood vessels (BVs), smooth muscle cells (SMCs), collagen fibers (CFs)) to form a three-dimensional (3D) network through their elongated cytoplasmic projections, emphasizing their involvement in numerous functions^{1-3,5,7,11,13-15}. In the past few years, TC distribution has been studied extensively in various organs (e.g., epicardium⁴, uterus⁵, fallopian tube⁶, placenta⁷, pancreas⁸, parotid gland⁹, skin¹⁰, urinary bladder¹¹, myocardium¹³, neuromuscular spindles¹⁴, lungs¹⁵, gallbladder¹⁶ and GIT^{12,17-21}) of single-stomach animals, but few studies have been done within the rumen of ruminants.

The rumen is a significant chamber of the complex stomach in ruminants that mainly acts as a food stirrer and fermenter. Its specific structure and function play an important role in the digestion and absorption of nutrients²². Previous studies of the GIT have focused primarily on the microorganisms and epithelial cells involved in nutrient digestion and uptake²²⁻²⁵. However, in recent years, gastrointestinal functional disorders associated with regulation between the enteric nervous system (ENS) and SMCs, such as rumen impaction and rumen flatulence, have had a tremendous effect on stock breeding²⁶⁻²⁹ and further research is needed. Wood and Furness proposed the concept of "neurogastroenterology," implying that mainly the ENS regulates the contraction and diastolic functions of smooth muscles^{30,31}. In recent years, new types of interstitial cells such as TCs have been carefully described in the GIT of rats^{17,18} and humans^{12,19-21}. In the muscle layer, TCs are involved in maintaining intestinal structural and dynamic stability. Research shows that TCs might even play an important role in the interaction between neurons and SMCs^{14,17,18,32}, expanding a new field for the advancement of gut diseases. Vannucchi et al. proposed that TCs might also play a role in transmitting slow waves in the GIT of mammals^{33,34}. Based on their intimate interaction with other structures (NFs, SMCs, BVs and CFs, neuromuscular spindles, immune cells, endothelial cells), TCs might also be involved in numerous physiological processes, including structural support, neurotransmission, intercellular communication, neo-angiogenesis regeneration as well as myocardial regeneration^{1-3,5,7,11,13-15,35-37}. Therefore, the existence of TCs in the rumen of ruminants, and their relationships with other structures, eagerly await investigation. This may provide new ideas for understanding digestion and nutrient absorption, as well as the diagnosis and treatment of gastrointestinal diseases in ruminants.

In the present study, we first confirmed, by transmission electron microscopy (TEM) and IF, that TCs are present in the muscle layers of the rumen. Close relationships between TCs and other structures (smooth muscle bundles, nerve tracts, BVs, SMCs, NFs, CFs and ganglionic neurons) were also detected. Our results will help to understand future research into the phenotype, ultrastructure and potential function of TCs in ruminants.

Materials and Methods

Animals

Four adult *Capra hircus* (goats) were used in this study. All goats were obtained from a commercial farm and managed in a traditional control and treatment manner. Animals were deeply anesthetized using IV administration of sodium thio-pental (10 mg/kg) and euthanized by means of an intracardiac injection of Tanax (0.5 ml/kg). Rumen samples were taken from the goats immediately following euthanasia. The tissues were collected immediately, placed in 10% neutral buffered formalin for fixation overnight, and then embedded in paraffin wax. Sectioning was performed at 5 µm. Sample preparation was conducted according to accepted international standards.

Transmission Electron Microscopy

The specimens were cut into small parts (1 mm³) and then immersed in 2.5% glutaraldehyde in PBS (4°C, pH 7.4, 0.1 mol/L) for 24 h. Tissues were rinsed in the same PBS and then post-fixed for 60 min at room temperature in the same way using buffered 1% osmium tetroxide (Polysciences Inc. Warrington, PA, USA) and washed in the buffer. The samples were then dehydrated in ascending concentrations of ethyl alcohol, infiltrated with a propylene oxide-Araldite mixture, and then embedded in Araldite. The blocks were then sectioned using an ultramicrotome (Reichert Jung, Wien, Austria), and ultrathin sections (50 nm) were mounted on copper-coated grids. The pieces were stained with 1% uranyl acetate and Reynold's lead citrate for 20 min.

Double-Labeling Immunofluorescence

In double immunofluorescence experiments, the paraffin sections were incubated overnight at 4°C with the following antibody pairs: mouse anti-vimentin (1:100) (Boster BioTechnology, Wuhan, China)/rabbit anti-CD34 (1:100) (Boster BioTechnology); mouse anti-vimentin(1:100) (Boster BioTechnology)/rabbit anti-PGP9.5 (1:100) (Boster BioTechnology); mouse anti-PGP9.5 (1:100) (Arigo, Taiwan, China)/rabbit anti-CD34 (1:100) (Boster BioTechnology). Following primary antibody application, all samples were incubated with anti-mouse Alexa Fluor 488 (1:200) (Life Technologies, Molecular Probes, Grand Island, NY, USA)/anti-rabbit rhodamine (1:200) (Life Technologies, Molecular Probes) for another 1.5 h at 37°C prior to rehydration in

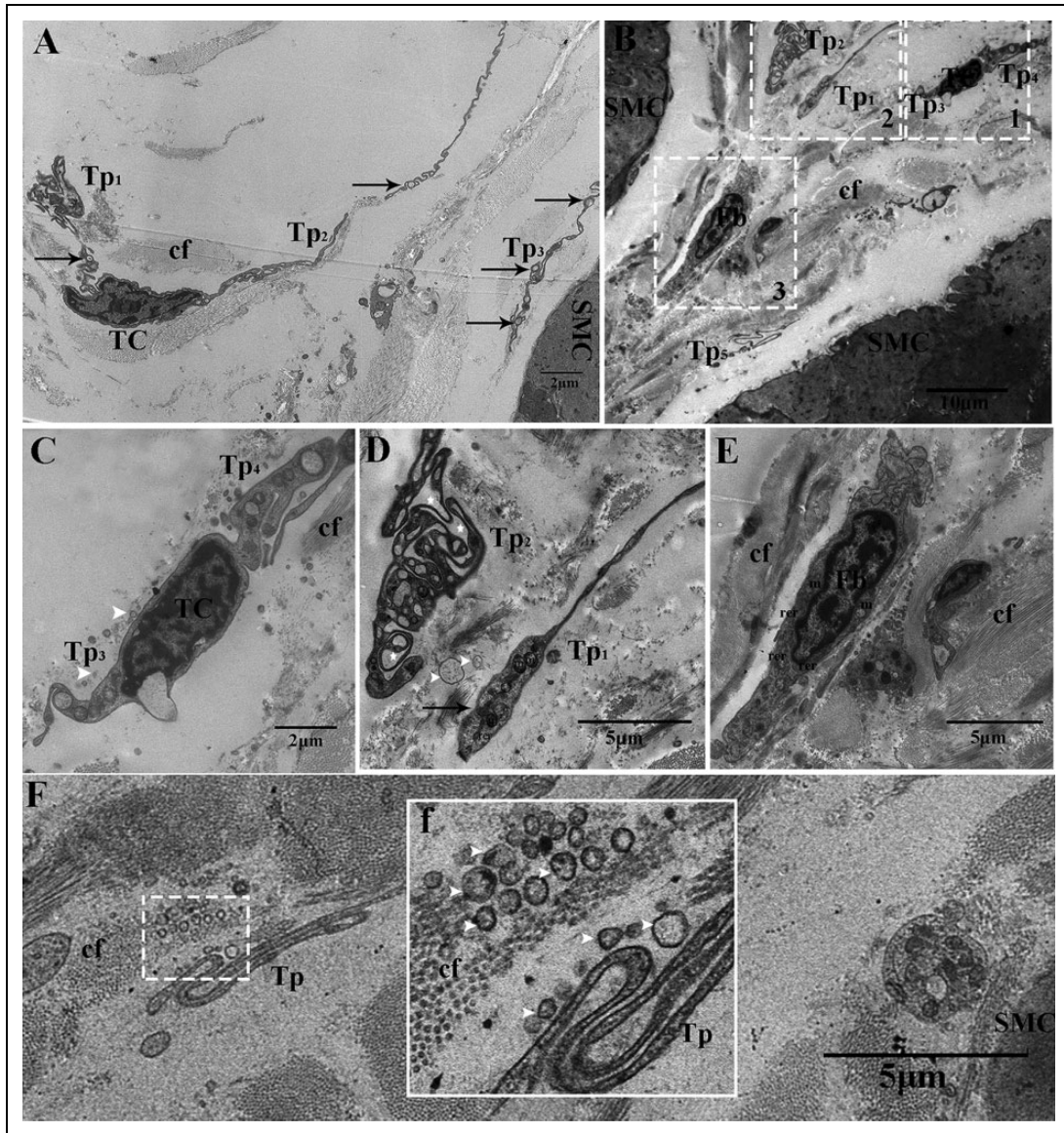


Fig 1. TEM images of the myenteric plexus of the goat rumen. (A) A typical TC, with a small stellate-shape cell body and two long beaded-like telopodes, harboring alternating podomers or podoms (arrows). TCs, several telopodes and a fibroblast located in the intermuscular connective tissue. Square-marked areas 1, 2, 3 in (B) are enlarged in (C, D, E), respectively. (C) Small bubbles (arrowheads) near a spindle-shape TC-MY. (D) Mitochondria and RER were observed in the podom of telopode₁. Small buttonholes (stars) composed of the telopode₂ convolutions. EVs (arrowheads) were present between two close telopodes. (E) A typical fibroblast. Square marked area in (F) is enlarged in (f), EVs (arrowhead) near the telopodes and CFs. The arrows indicate podoms. TC: telocyte; Tp₁₋₅: telopode₁₋₅; rer: rough endoplasmic reticulum; m: mitochondria; SMC: smooth muscle cell; cf: collagen fiber; Fb: fibroblast. Bar = 2 μm in A, C; Bar = 10 μm in B; Bar = 5 μm in D, E, F.

PBS. The sections were then incubated with 4',6-diamidino-2-phenylindole (DAPI; Life Technologies, Molecular Probes) and then stimulated under a fluorescent microscope. Pictures of each specimen section were sampled at 40–400x magnification.

Equipment

For light microscopy, all specimens were initially subjected to LED light to visualize fluorescence under an Olympus

DP73 microscope (Guangzhou City, Guangdong Province, China. For TEM, the sections were examined and photographed with an H-7650 transmission electron microscope (Hitachi Suzhou City, Hong Kong).

Results

In the muscle layer of goat rumen, TCs were distributed in the myenteric plexus (TC-MYs) (Fig. 1; Fig. 2; Fig. 3), between the circular and the longitudinal muscle layers, and

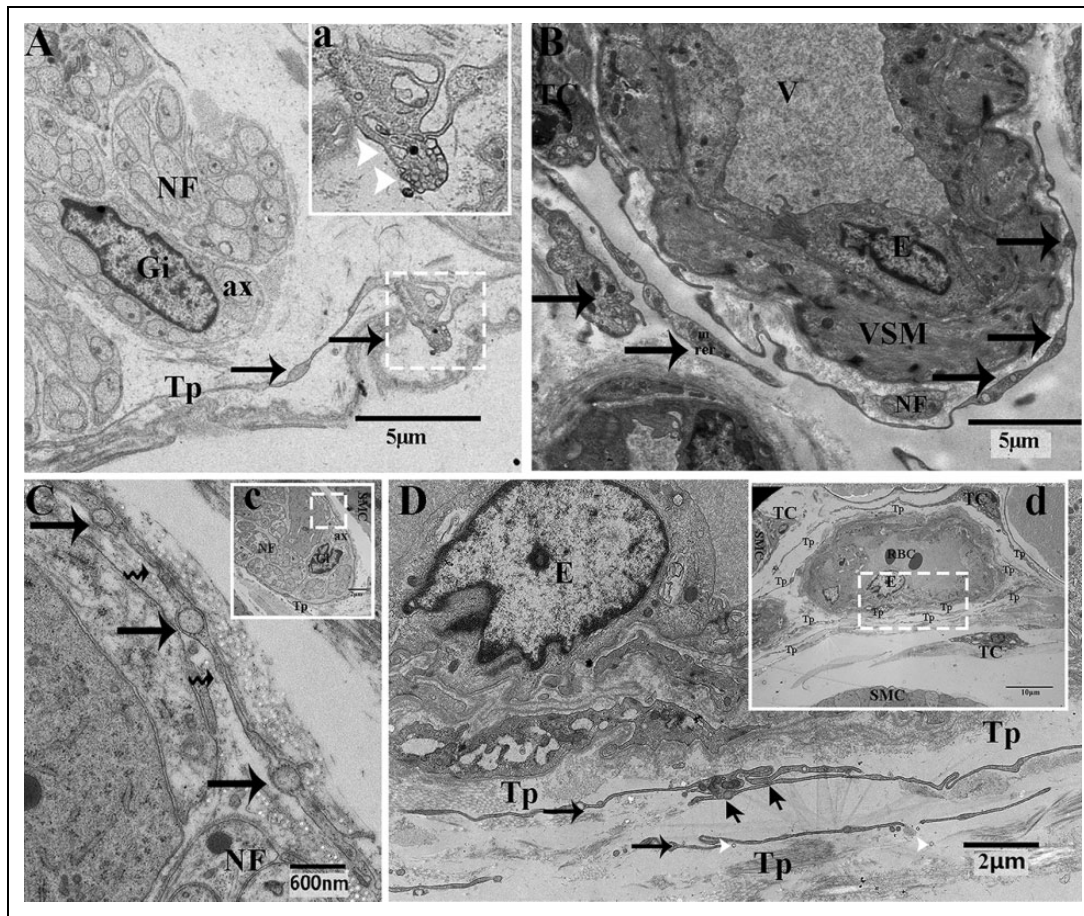


Fig 2. TCs surrounding the nerve tracts and BVs in the myenteric plexus of the goat rumen. Square marked areas in (A, c, d) are enlarged in (a, C, D), respectively. (A, c) Telopodes were closely surrounding the nerve tract, where each axon were embedded by the cytoplasm of the glial cells. (a) The podom shedding multivesicular cargos (arrowheads). (B) TCs in the vicinity of an arteriole wall, near a small NF. (C) A typical beaded-like telopode with several caveolae (bent arrows). (d) Numerous TCs and telopodes surrounded the BVs forming a network. (D) Homotypic connections between the two telopodes (diagonal arrows). EVs (arrowheads) close to telopodes. The arrows indicate podoms. TC: telocytes; Tp: telopode; rer: rough endoplasmic reticulum; m: mitochondria; VMA: vessels smooth muscle cell; E: endothelial cell; V: blood vessels; RBC: red blood cell. Gi: glial cells; ax: axon; NF: nerve fiber. Bar = 5 μ m in A, B; Bar = 600 nm in C; Bar = 2 μ m in D.

within the circular and longitudinal muscle layer (TC-CMs and TC-LMs) (Fig. 4). A typical TC-MY displayed a stellate-shape cell body (Fig. 1A) and two extremely long and thin prolongations called telopodes, and, alternately, thin segments (podomer) or dilation segments (podom). TC-MYs and their telopodes gathered in the intermuscular connective tissue (Fig. 1B). Small bubbles appeared around a spindle-shape TC-MY (Fig. 1C). Extracellular vesicles (EVs) of different sizes were observed in the vicinity of telopodes (Fig. 1D–F(f)). Telopode₂ formed a labyrinthine apparatus with a very convoluted profile, while telopode₁ harbored flexion- and irregularity-free surfaces (Fig. 1D). A typical fibroblast has a rich cytoplasm with expansive rough endoplasmic reticulum (RER) (Fig. 1E). TC-MYs are frequently wrapped around nerve tracts, where each axon is embedded in the cytoplasm of the glial cells (Fig. 2A(c)), as well as around the intermuscular BVs (Fig. 2B(d)). Notably, the podom released multivesicular cargos within the

intercellular matrix (Fig. 2A). TC-MYs were close to an arteriole wall, near small NFs (Fig. 2B). The telopodes appeared as typical bead-like shapes with several caveolae, surrounding the nerve bundle (Fig. 2C). Moreover, numerous TC-MYs, as well as their telopodes, formed a network by the homojunctions (Fig 2D) surrounding the BVs (Fig 2D). A network of TC-MYs was also established in the neighborhood of the smooth muscle bundle and the nerve tract (Fig. 3A), by homojunctions Tp₁–Tp₂ (Fig. 3B), Tp₂–Tp₃ (Fig. 3C), Tp₂–Tp₅ (Fig. 3D), Tp₂–Tp₄ (Fig. 3E), and heterojunctions between Tp₂ and CFs (Fig. 3C). Interlocking structures also occurred between telopodes (Fig. 3B, E). EVs were budding from the cytoplasm of the telopodes (Fig. 3C–E). Both TC-CMs and TC-LMs bordered the bundles of smooth muscle with their fairly long or repeatedly curled processes. (Fig. 4A, B). They were also close to the NFs and/or SMCs in intimate interaction (Fig. 4B,C,E(e)), but no gap junction was found. In addition, multivesicular

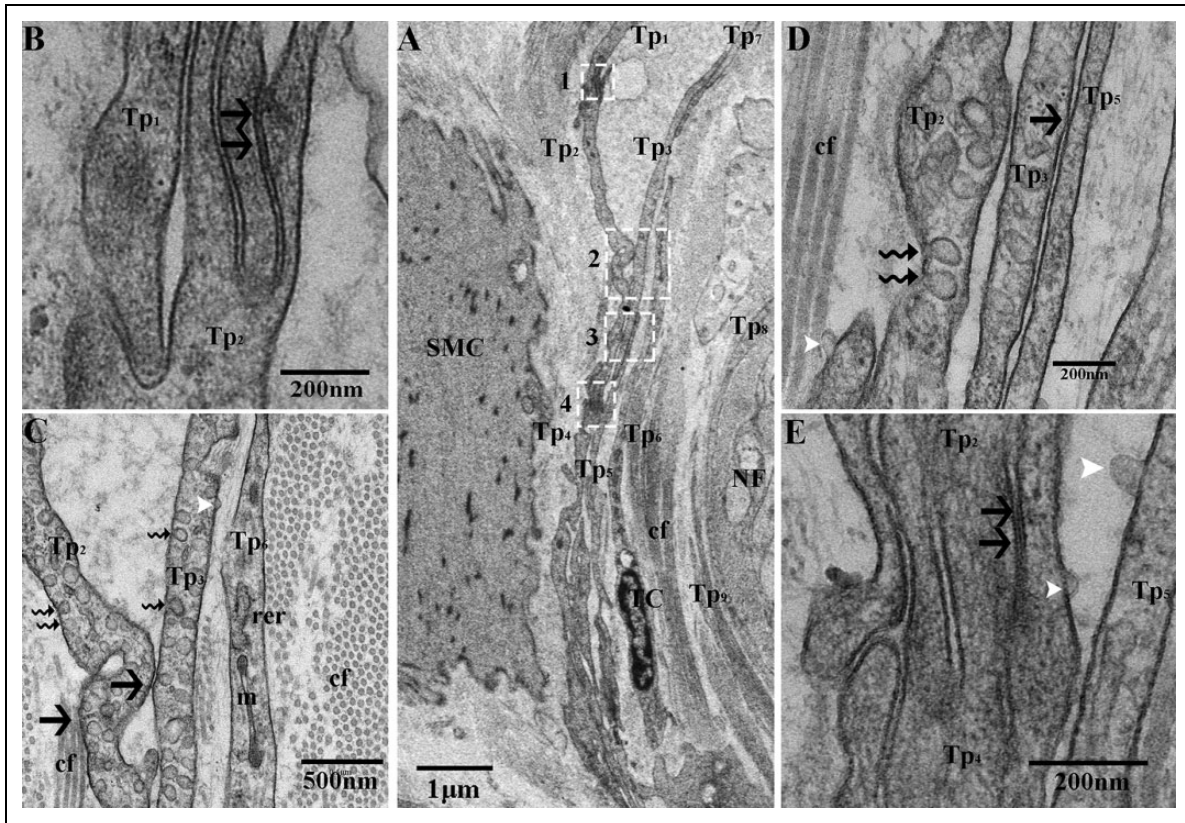


Fig 3. TEM of homo- and heterojunctions in the myenteric plexus of the goat rumen. (A) At least nine telopodes were located in the intermuscular connective tissue, one side close to the nerve bundle and the other side near the muscle bundle. Square marked-areas 1, 2, 3, 4 in (A) are enlarged in (B, C, D, E). The homojunctions (arrows) were visible between telopodes: Tp_1 - Tp_2 (B), Tp_2 - Tp_3 (C), Tp_2 - Tp_5 (D), Tp_2 - Tp_4 (E). (B, E) Interlocking structure between telopodes. (C) Heterojunction (arrow) observed between the telopode and CFs. (B, C, E) EVs (arrowhead) budding from the cytoplasm of telopodes. (C, D) Bent arrows indicate caveolae. TC: telocyte; Tp_{1-9} : telopode $_{1-9}$; rer: rough endoplasmic reticulum; m: mitochondria; SMC: smooth muscle cell; cf: collagen fiber; NF: nerve fiber. Bar = 1 μ m in A; Bar = 200 nm in B, D, E; Bar = 500 nm in C.

bodies (MVBs) were present in the cytoplasm of podoms (Fig. 4D). EVs were also observed between NFs and the telopodes (Fig. 4E).

The presence of TCs was also confirmed by immunolabeling of CD34+/vimentin+ cells (Fig. 5). Vimentin was expressed mainly in the cytoplasm, while CD34 was expressed in the cytomembrane. These positive cells (TC-MYs, TC-CMs, and TC-LMs) covered the entire muscular layers, surrounding the intermuscular ganglion, the intermuscular BVs as well as the entire smooth muscle bundles (Fig. 5A(a)–C(c)) to form a network (Fig. 5A–C). In the myenteric connective tissue, TC-MYs were clusterly distributed and interweaved with each other, forming a network (Fig. 6A–C). In the ganglion, three cell types were explored: Vimentin+/CD34+ cells displaying TCs characteristics (TC-MYs) (Fig. 7A–C); Vimentin+/CD34- glial cells interconnected to form ring-boundary layers (Fig. 7B, E); and PGP9.5+ neurons and NFs (Fig. 7D(d₁) and Fig. 7D(d₂)). Each ganglionic neuron was encircled by a ring-boundary layer consisting of several glial cells (Fig.

7F(f₁)) and TC-MYs were located in the periphery of the glial cells ring-boundary layer and close to the neurons (Fig. 7C(c)). Several NFs were surrounded by the cytoplasm of glial cells (Fig. 7F(f₂)). At low magnification, it was found that the network of TC-MYs was centered on ganglia, wrapping around the ganglionic neurons, as well as spreading to surround the muscle layers (Fig. 7G–I). A group of TC-MYs and telopodes were interwoven into a network, surrounded the BVs (Fig. 8A–C; Fig. 8A(a)–C(c)). TC-CMs clustered in the interstitial space between the smooth muscle bundles, and were seemingly wrapped around the whole smooth muscle bundle (Fig. 9A–C). The same results were observed for TC-LMs (Fig. 10A–C). At high magnification, TCs were characterized specifically as spindle-shaped (Fig. 6A(a)–C(c) and Fig. 10A(a)–C(c)) and triangular- (Fig. 9A(a)–C(c)) cells with a nucleus and several elongated bead-like projections, which was consistent with our TEM analysis. Notably, podoms were labeled as obvious bright spots (Fig. 7C(c); Fig. 8C(c); Fig. 9C(c); Fig. 10C(c)).

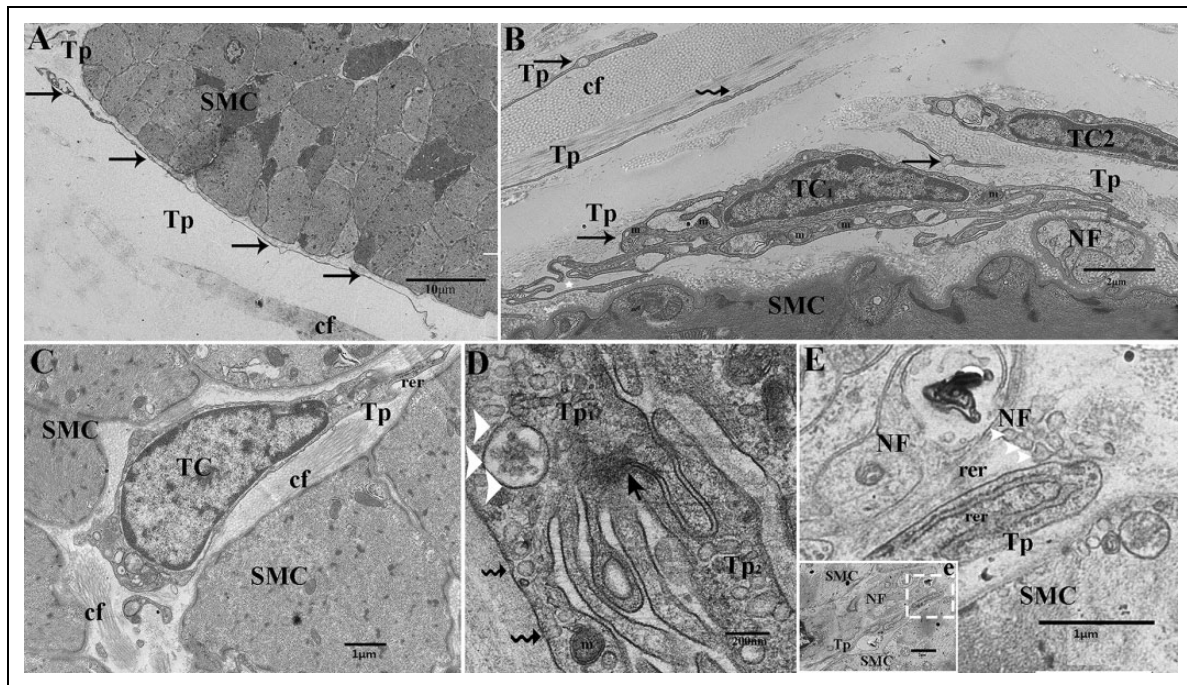


Fig 4. Intimate relationships between TCs and other structures (smooth muscle bundles, SMCs, NFs and CFs) in the circular and longitudinal muscle layers of the goat rumen. (A) A fairly long telopode bordering the smooth muscle bundles. (B) A triangle-shaped TC with two long and repeatedly curled processes, close to NFs and SMCs. Several moniliform telopodes were embedded in CFs. (C) A spindle-shaped TC close to SMCs. (D) MVB (arrowheads), imaged in the cytoplasm of telopode₁. Homojunction between two telopodes. Rent arrows indicated caveolae. Square marked areas in (e) was enlarged in (E), EVs (arrowheads) in the vicinity of the NFs and SMCs. The arrows indicate podoms. TC: telocyte; Tp_{1,2}: telopode_{1,2}; rer: rough endoplasmic reticulum; m: mitochondria; SMC: smooth muscle cells; cf: collagen fiber; NF: nerve fibers; Bar = 10 μm in A; Bar = 2 μm in B; Bar = 1 μm in C, E; Bar = 200 nm in D.

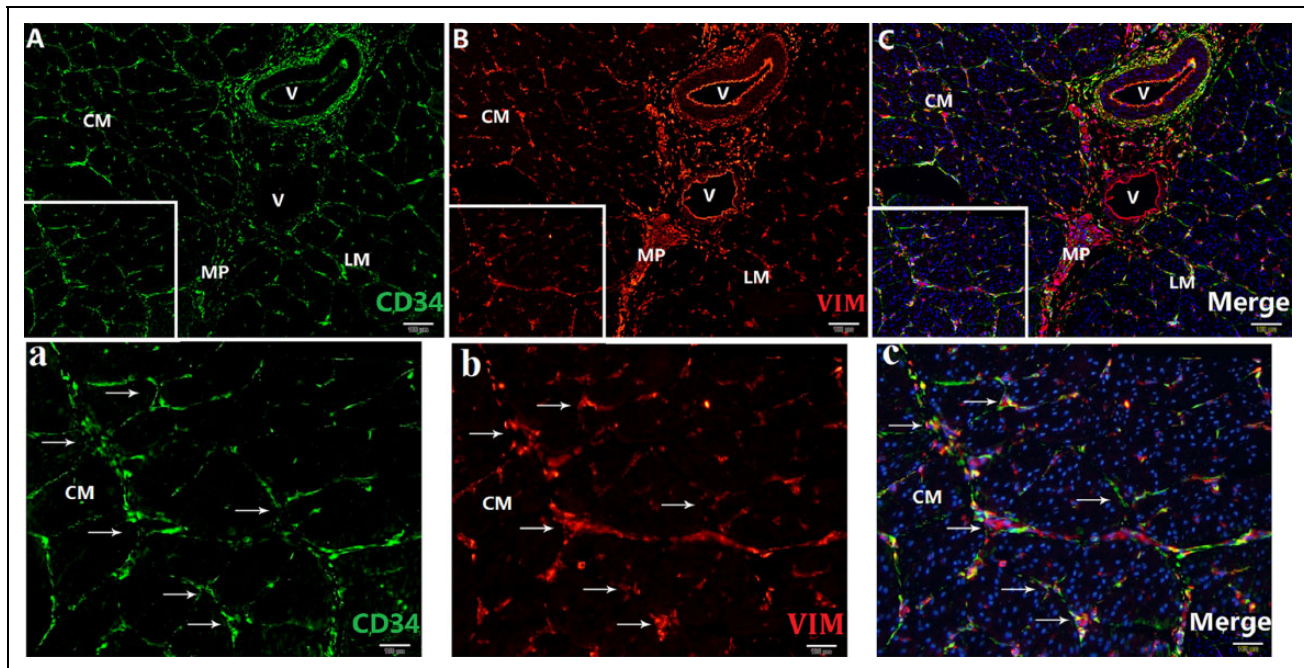


Fig 5. Double-immunofluorescence of CD34⁺ (green in A)/Vimentin⁺ (red in B) labeled TCs (C). TCs were abundantly distributed in the myenteric plexus (TC-MYs) and interconnected to form a complex network, as well as within the circular and longitudinal muscle layer (TC-CMs and TC-LMs). Square marked areas in (A, B, C) are enlarged in (a, b, c), respectively. (c) The TC-CMs clearly surrounded each smooth muscle bundle. V: BVs; CM: circular muscle layer; LM: longitudinal muscle layer; MY: myenteric plexus. Bar = 100 μm in A–C and a–c.

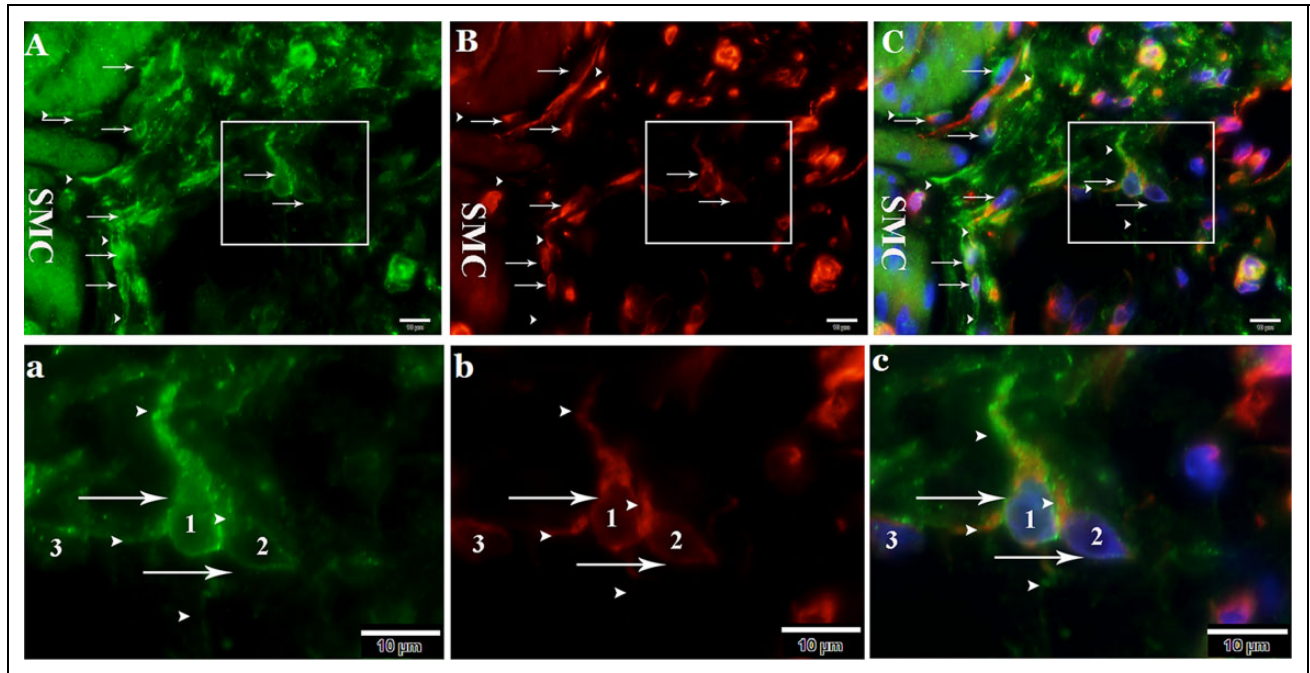


Fig 6. CD34+ (green in A)/Vimentin+ (red in B) labeled TC-MYs (C). TC-MYs were widely distributed in intermuscular connective tissue, forming a network. Square marked areas in (A, B, C) are enlarged in (a, b, c), respectively. (a–c) The spindle-shaped TC₁ with two long processes was close to both TC₂ and TC₃. Nucleus (arrows) and processes (arrowheads). SCM: smooth muscle cells. Bar = 10 μm in A–C, a–c.

Discussion

In the GIT of monogastric animals, TCs have been regarded as a new cell type, different from other interstitial cells^{1,17,18,37}. By using traditional TEM methods and the most recommended immunolabeling markers, the present study shows, for the first time, the existence of TCs in the rumen muscle layers. Ultrastructurally, TC morphology in the goat rumen was similar to that described in previous reports on single-stomach animals such as the rabbit jejunum human urinary tract^{12,17,38}. TC has a small cell body with several long and thin cellular projections (called telopodes). Telopodes display thin segments (podomers) and dilated segments (podoms). Podoms contained mitochondria, RER and caveolae. Ultrastructurally, we distinguished the TCs and fibroblasts in this study. As previously reported, fibroblasts appeared short with thick projections, and their cytoplasm contained extensive RER^{6,35,39}. In addition, we used IF—a fairly reliable method—to demonstrate that TCs in the muscle layers of goat rumen, like TCs in other locations, were labeled as CD34+/Vimentin+ cells^{4,15,40}. Moreover, Vannucchi et al. established that TCs in the human GIT can be identified by CD34/PDGFR, while being negative for c-kit/CD117, making TCs and c-kit-positive interstitial cells of Cajal (ICC) clearly distinguishable¹². However, in our study, some differences could be observed. Vimentin (mesenchymal cell marker, cytoplasmic protein) was expressed mainly in the cell body and only rarely in the prolongations. On the

other hand, CD34 (hematopoietic stem cell marker, membrane protein) was expressed almost everywhere, even in the fine segments of telopodes where vimentin expression was almost negligible. This may be due to the telopode, especially its fine segments, containing little cytoplasm. In addition, our other results also supported this hypothesis: Vimentin could be expressed strongly in the prolongations of glial cells, but extremely weakly within telopodes. Remarkably, some bright spots were detected on the long and slender projections of TCs, indicating podomes.

The role of TCs has not yet been unraveled, although various speculations have been made. TCs are considered as a new cell-type due to their long and bead-like prolongations allowing interaction with themselves via homojunctions. These cells can also interact with other structures through heterojunctions, thus constituting a 3D-network that may be related to structural support as well as intercellular signaling locally, or, at a longer distance, directly or indirectly through the TC network^{4,6,9,37}. Specifically, TC networks were reduced or even completely absent around smooth muscle bundles and myenteric plexus ganglia under conditions of disease such as ulcerative colitis¹⁹, Crohn's disease²⁰ as well as systemic sclerosis²¹, emphasizing the importance of the TC network from the reverse side. As mentioned above, these hypotheses are consistent with our experimental results. In addition, the data reported here also illustrate that TCs significantly surround rumen-nerve tracts, smooth muscle bundles and BVs. This

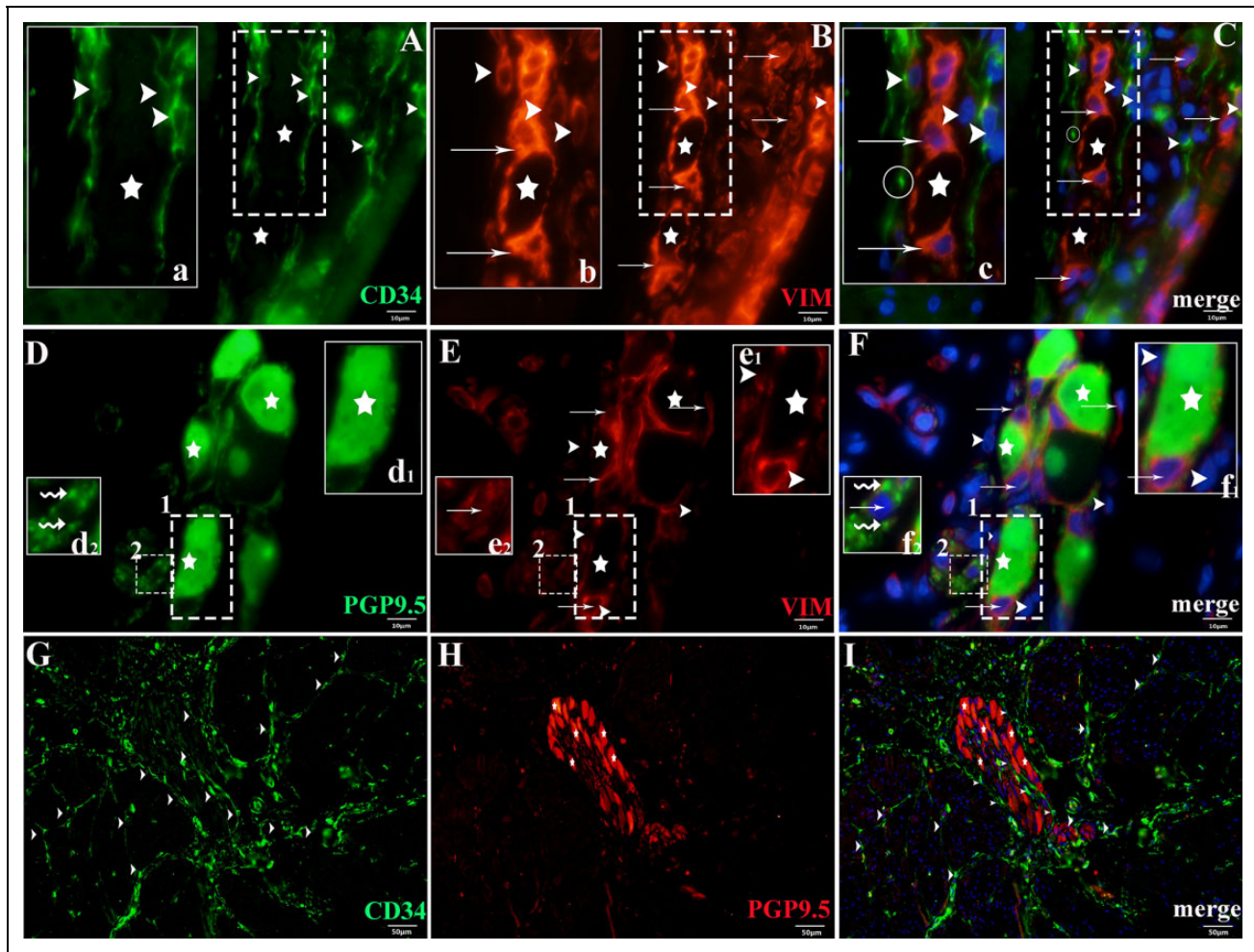


Fig 7. Close relationship between TC-MYs, glial cells, ganglionic neurons and NFs. Square marked areas in (A–C; D_{1,2}; E_{1,2}; F_{1,2}) are enlarged in (a–c; d_{1,2}; e_{1,2}; f_{1,2}), respectively. TC-MYs were visible as CD34+/Vimentin+ cells (arrowheads), whereas glial cells displayed vimentin +/CD34- cells profile (arrows). PGP9.5 was used as a neurospecific marker for neurons (stars) and NFs (bent arrow) labeling. (a–c) TC-MYs close to the ring-boundary composed of several glial cells. (d₁–f₁) The ring-boundary of glial cells encircled each ganglionic neurons. (d₂–f₂) The cytoplasm of the glial cells embedding the small NFs. (G–I) Cluster distribution of TC-MYs with interweaving structure and wrapping around the ganglionic neurons and smooth muscle bundles. (c) A bright spot showing podom (circle). Bar = 10 μm in A–F; Bar = 20 μm in G–I.

characteristic has also been extensively reported in single-stomach animals^{1–3,5,7,11–15}. In particular, TCs located in the internal and external surfaces of ganglia, surrounding ganglionic neurons, follow the glial cells layer as well as encompassing the entire ganglion, respectively. TCs-glial cells-ganglionic neurons may form an functional units regulating the microenvironment of the myenteric plexus^{14,32,41}.

Popescu and Fausone-Pellegrini suggested that TCs are involved in intercellular signaling by secreting small signal molecules (e.g., proteins or RNAs, microRNA included) and by shedding microvesicles within the extracellular matrix¹. Furthermore, this function was also proposed to occur in the myocardium^{35,42}. A series of results evidenced the importance of EVs in TCs-mediated intercellular communication^{1,35,42,43}. It has been shown that TCs can release

extracellular vesicles into the stromal space of different organs^{1,35,42,43}. Studies revealed that the extracellular vesicles were frequently derived from projections^{1,35,42,43} and rarely from the body of TC in culture⁴⁴. However, the extracellular vesicles observed in this study were released only by the telopodes in the muscle layers of the goat rumen. A possible explanation is that these observations are influenced by the section angle and the sites of sample cutting. Fertig et al. described that cardiac TCs in culture release extracellular vesicles of different sizes: exosomes (45 ± 8 nm), ectosomes (128 ± 28 nm) and multivesicular cargos (1 ± 0.4 μm)⁴⁴. In the present work, the secretory vesicles were observed both in the intracellular of telopodes and within extracellular space between telopodes and telopodes, NFs, SMCs as well as CFs. Extracellular vesicles were found in the vicinity of the telopodes, near the NFs, SMCs and CFs, or

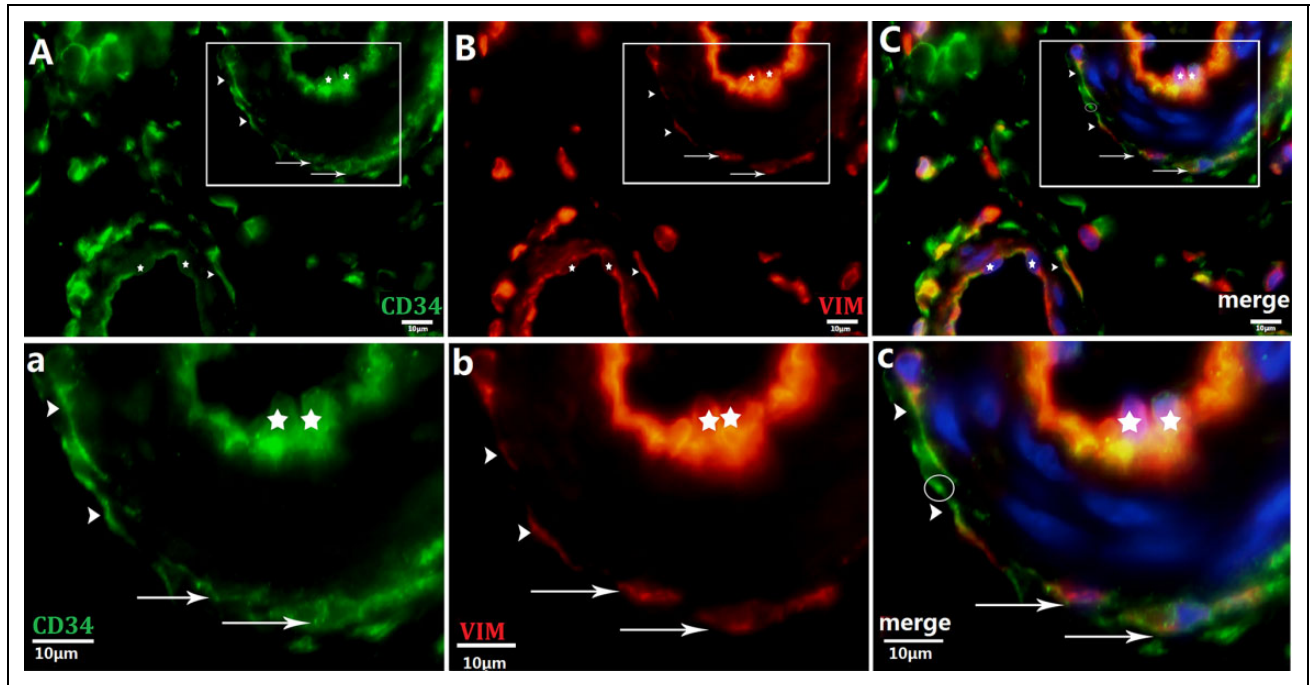


Fig 8. CD34+ (green in A)/Vimentin+ (red in B) labeled TC-MYs (C), surrounding the BVs. (a, b, c) A group of TC-MYs and telopodes forming a network around the BVs. Square marked areas in (A, B, C) are enlarged in (a, b, c), respectively. Nucleus (arrows), processes (arrowheads), vascular endothelial cells (white stars), podom (circle). Bar = 10 µm in A–C, a–c.

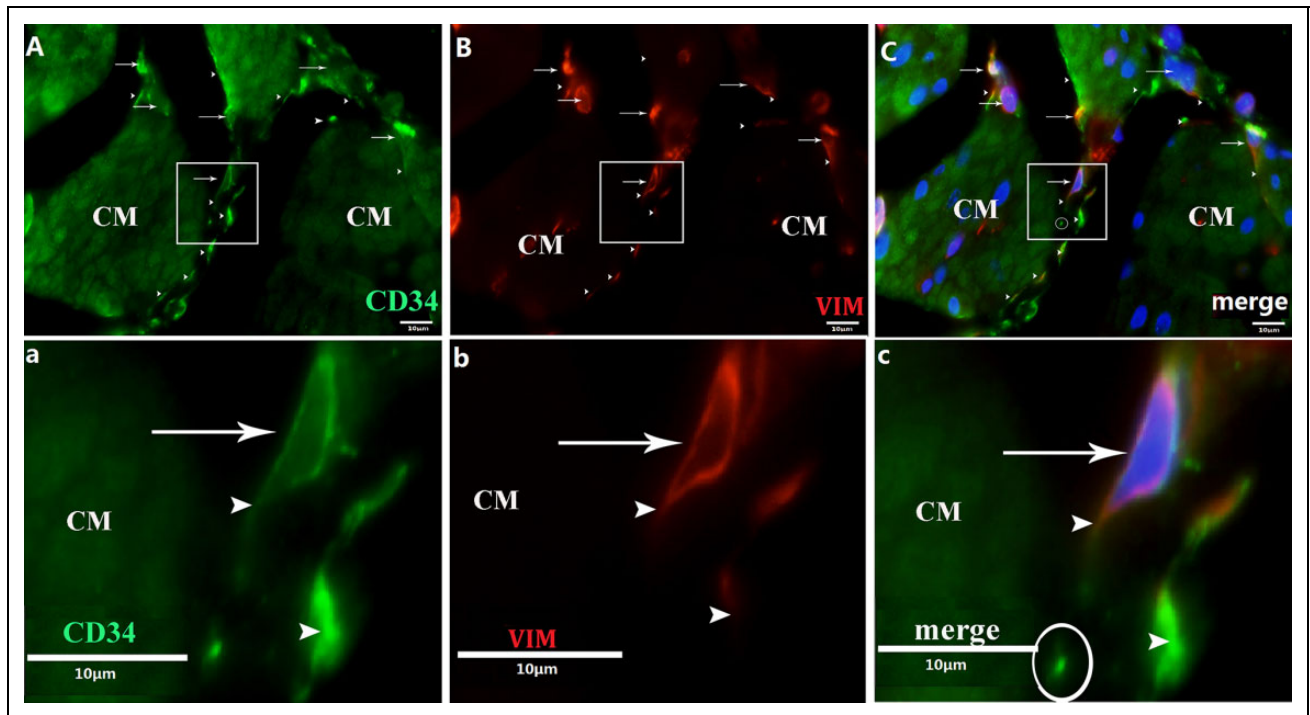


Fig 9. CD34+ (green in A)/Vimentin+ (red in B) labeled TC-CMs, bordering the whole smooth muscle bundles with long processes. (C) Square marked areas in (A, B, C) are enlarged in (a, b, c), respectively. (a–c) A triangular-shaped TC-CM with one process, near other telopodes. (c) A podom, marked as a bright spot (circle). Nucleus (arrow) and processes (arrowhead). Bar = 10 µm in A–C, a–c.

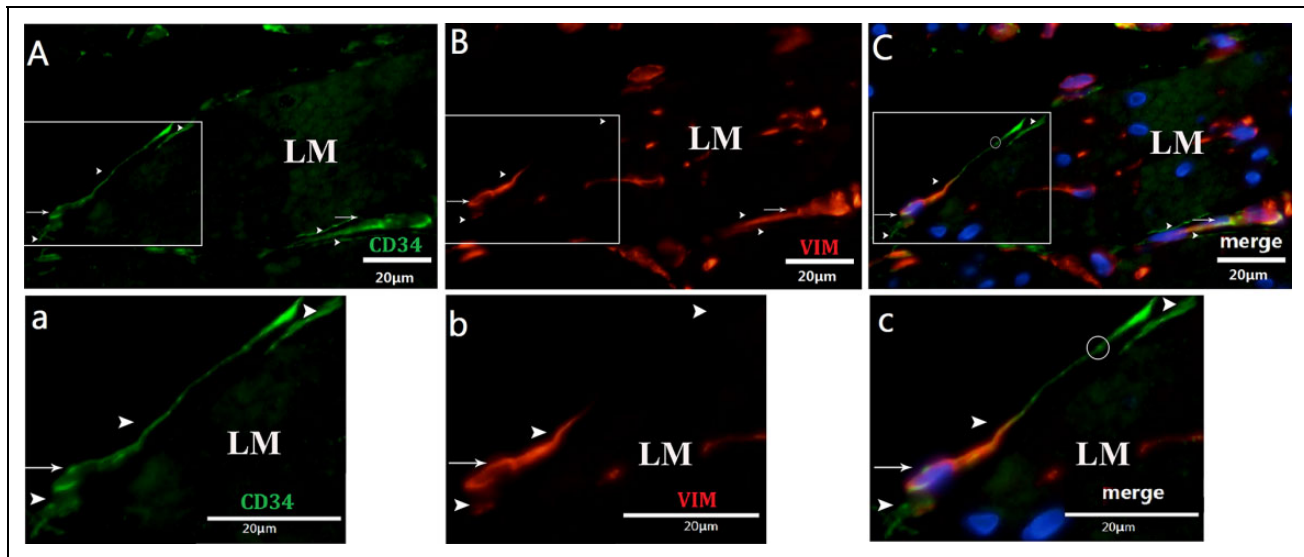


Fig 10. CD34⁺ (green in A)/Vimentin⁺ (red in B) labelled TC-LMs, around the smooth muscle bundles. Square marked areas in (A, B, C) are enlarged in (a, b, c), respectively. (a–c) A spindle-shaped TC with two long processes, close to other telopodes. (c) A podom, marked as a bright spot (circle). Nucleus (arrow) and process (arrowhead). Bar = 20 μ m in A–C, a–c.

as buds originating from the telopodes plasma membrane. On the other hand, MVBs were observed in the cytoplasm of telopodes. Interestingly, some multivesicular cargos were released from telopodes, close to NFs. Based on these findings, we hypothesize that telopode shape may be responsible for the delivery of secretory vesicles to the extracellular matrix, contributing to intercellular communication between telopodes and telopodes, NFs, SMCs as well as CFs, either locally or over a longer distance.

Conclusion

The results of this study indicate that TCs are present in abundance in the muscle layers of the goat rumen and establish close connections with telopodes and other rumen structures (ganglion neurons, nerve bundles, BVs, CFs, NFs, and SMCs). Intracellular and extracellular secretory vesicles from TCs were also observed. On the basis of their distribution and morphology, we suggest that TCs may be involved in structural support and intercellular communication between TCs and telopodes as well as the other rumen structures. This study provides new perspectives for understanding digestion in ruminants as well as the associated nutrient absorption. However, further studies are required to decipher the underlying mechanisms.

Ethical Approval

This study was approved by the Animal Ethics Committee of Nanjing Agricultural University, China.

Statement of Human and Animal Rights

All experiments were conducted according to the “Guidelines on Ethical Treatment of Experimental Animals” by the Jiangsu Provincial People’s Government (SYXK (SU) 2010-0005).

Statement of Informed Consent

There are no human subjects in this article and informed consent is not applicable.

Declaration of Conflicting Interests

The author(s) declared no potential conflicts of interest with respect to the research, authorship, and/or publication of this article.

Funding

The author(s) disclosed receipt of the following financial support for the research, authorship, and/or publication of this article: This work was supported by the grants from National Key Research and Development Plan (No.2018YFD0501902), the Fundamental Research Funds for the Central Universities of China (No. Y0201700174), the National Natural Science Foundation of China (No. 31772688 and No. 31402155), China Postdoctoral Science Foundation Funded Project (No. 2016M591861), the Priority Academic Program Development of Jiangsu Higher Education Institutions, China.

References

1. Popescu LM, Faussonpellegrini MS. TELOCYTES – a case of serendipity: the winding way from Interstitial Cells of Cajal (ICC), via Interstitial Cajal-Like Cells (ICLC) to TELOCYTES. *J Cell Mol Med.* 2010;14(4):729–740.
2. Fausson-Pellegrini MS, Popescu LM. Telocytes. *Biomol Concepts.* 2011;2(6):481–485.
3. Cretoiu SM, Popescu LM. Telocytes revisited. *Biomol Concepts.* 2014;5(5):353–369.
4. Popescu LM, Manole CG, Gherghiceanu M, Ardelean A, Nicolescu MI, Hinescu ME, Kostin S. Telocytes in human epicardium. *J Cell Mol Med.* 2010;14(8):2085–2093.
5. Cretoiu SM, Cretoiu D, Marin A, Radu BM, Popescu LM. Telocytes: ultrastructural, immunohistochemical and

- electrophysiological characteristics in human myometrium. *Reproduction*. 2013;145(4):357–370.
6. Popescu LM, Ciontea SM, Cretoiu D, Hinescu ME, Radu E, Ionescu N, Ceausu M, Gherghiceanu M, Braga RI, Vasilescu F, Zagrean L, Ardeleanu C. Novel type of interstitial cell (Cajal-like) in human fallopian tube. *J Cell Mol Med*. 2005;9(2):479–523.
 7. Suciul L, Popescu LM, Gherghiceanu M, Regalia T, Nicolescu M I, Hinescu ME, Faussone-Pellegrini MS. Telocytes in human term placenta: morphology and phenotype. *Cells Tissues Organs*. 2010;192(5):32–39.
 8. Zhang H, Yu P, Zhong S, Ge T, Peng S, Guo X, Zhou Z. Telocytes in pancreas of the Chinese giant salamander (*Andrias davidianus*). *J Cell Mol Med*. 2016;20(11):5.
 9. Nicolescu MI, Bucur A, Dinca O, Rusu MC, Popescu LM. Telocytes in parotid glands. *Anat Rec*. 2012;295(3):378–385.
 10. Ceafalan L, Gherghiceanu M, Popescu LM, Simionescu O. Telocytes in human skin—Are they involved in skin regeneration? *J Cell Mol Med*. 2012;16(7):1405–1420.
 11. Vannucchi MG, Traini C, Guasti D, Popolo DG, Faussone-Pellegrini MS. Telocytes subtypes in human urinary bladder. *J Cell Mol Med*. 2014;18(10):2000–2008.
 12. Vannucchi MG, Traini C, Manetti M, Manneschi IL, Faussone MS. Telocytes express PDGFR α in the human gastrointestinal tract. *J Cell Mol Med*. 2013;17(9):1099–1108.
 13. Gherghiceanu M, Popescu LM. Heterocellular communication in the heart: electron tomography of telocyte-myocyte junctions. *J Cell Mol Med*. 2011;15(4):1005–1011.
 14. Díaz-Flores L, Gutiérrez R, Sáez FJ, Díaz-Flores LJ, Madrid JF. Telocytes in neuromuscular spindles. *J Cell Mol Med*. 2013;17(4):457–465.
 15. Yang Y, Sun W, Wu SM, Xiao J, Kong X. Telocytes in human heart valves. *J Cell Mol Med*. 2014;18(5):759–765.
 16. Pasternak A, Gajda M, Gil K, Matyja A, Tomaszewski KA, Walocha JA, Kulig J, Thor P. Evidence of interstitial Cajal-like cells in human gallbladder. *Folia Histochem Cytobiol*. 2012;50(4):581–585.
 17. Cretoiu D, Cretoiu SM, Simionescu AA, Popescu LM. Telocytes, a distinct type of cell among the stromal cells present in the lamina propria of jejunum. *Histol Histopathol*. 2012;27(7):1067–1078.
 18. Cantarero CI, Luesma BJ, Junquera EC. Identification of telocytes in the lamina propria of rat duodenum: transmission electron microscopy. *J Cell Mol Med*. 2011;15(1):26–30.
 19. Manetti M, Rosa I, Messerini L, Manneschi IL. Telocytes are reduced during fibrotic remodelling of the colonic wall in ulcerative colitis. *J Cell Mol Med*. 2015;19(1):62–73.
 20. Milia AF, Ruffo M, Manetti M, Rosa I, Conte D, Fazi M, Messerini L, Manneschi IL. Telocytes in Crohn's disease. *J Cell Mol Med*. 2013;17(12):1525–1536.
 21. Manetti M, Rosa I, Messerini L, Guiducci S, Matucci CM, Manneschi IL. A loss of telocytes accompanies fibrosis of multiple organs in systemic sclerosis. *J Cell Mol Med*. 2014;18(2):253–262.
 22. Ternouth JH. The rumen and its microbes. *Aust Vet J*. 1968;44(2):47.
 23. Sakata T, Tamate H. Rumen epithelium cell proliferation accelerated by propionate and acetate. *J Dairy Sci*. 1979;62(1):49–52.
 24. Abdoun K, Stumpff F, Martens H. Ammonia and urea transport across the rumen epithelium: a review. *Anim Health Res Rev*. 2006;7(1–2):43–59.
 25. Shen H, Lu Z, Xu Z, Shen Z. Diet-induced reconstruction of mucosal microbiota associated with alterations of epithelium lectin expression and regulation in the maintenance of rumen homeostasis. *Sci Rep*. 2017;7(1):3941.
 26. Drossman DA. The functional gastrointestinal disorders and the Rome III process. *Gastroenterology*. 1999;130(5):1377–1390.
 27. Lgbokwe IO, Kolo MY, Egwu GO. Rumen impaction in sheep with indigestible foreign bodies in the semi-arid region of Nigeria. *Small Ruminant Res*. 2003;49(2):141–146.
 28. Wei C, Lin SX, Wu JL, Zhao G Y, Zhang TT, Zheng WS. Effects of supplementing Vitamin E on in vitro rumen gas production, volatile fatty acid production, dry matter disappearance rate, and utilizable crude protein. *Czech J Anim Sci*. 2015;60(8):335–341.
 29. Nezami BG, Srinivasan S. Enteric nervous system in the small intestine: pathophysiology and clinical implications. *Curr Gastroenterol Rep*. 2010;12(5):358–365.
 30. Wood JD, Alpers DH, Andrews PR. Fundamentals of neurogastroenterology. *Gut*. 1999;45(suppl 2):ii6–i16.
 31. Furness JB. The enteric nervous system and neurogastroenterology. *Nat Rev Gastroenterol Hepatol*. 2012;9(5):286–294.
 32. Bosco C, Diaz E, Gutierrez R, Gonzalez J, Perez J. Ganglionic nervous cells and telocytes in the pancreas of octodon degus extra and intrapancreatic ganglionic cells and telocytes in the degus. *Auton Neurosci*. 2013;177(2):224–230.
 33. Faussone MS. Interplay among enteric neurons, interstitial cells of Cajal, resident and not resident connective tissue cells. *J Cell Mol Med*. 2009;13(7):1191–1192.
 34. Vannucchi MG, Traini C. Interstitial cells of Cajal and telocytes in the gut: twins, related or simply neighbor cells? *Biomol Concepts*. 2016;7(2):93–102.
 35. Manole CG, Cismasiu V, Gherghiceanu M, Popescu LM. Experimental acute myocardial infarction: telocytes involvement in neo-angiogenesis. *J Cell Mol Med*. 2011;15(11):2284–2296.
 36. Gherghiceanu M, Hinescu ME, Andrei F, Mandache E, Macarie CE, Faussone-Pellegrini MS, Popescu LM. Interstitial Cajal-like cells (ICLC) in myocardial sleeves of human pulmonary veins. *J Cell Mol Med*. 2008;12(5):1777–1781.
 37. Rusu MC, Pop F, Hostiuc S, Curca GC, Jianu AM, Paduraru D. Telocytes form networks in normal cardiac tissues. *Histol Histopathol*. 2012;27(6):807–816.
 38. Gevaert T, De VR, Van DF, Joniau S, Van OJ, Roskams T, Ridder D. Identification of telocytes in the upper lamina propria of the human urinary tract. *J Cell Mol Med*. 2012;18(4):e105.
 39. Fields KL, Raine CS. Ultrastructure and immunocytochemistry of rat Schwann cells and fibroblasts in vitro. *J Neuroimmunol*. 1982;2(2):155–166.

40. Díaz-Flores L, Gutiérrez R, García MP, Sáez FJ, Díaz-Flores LJ, Valladares F, Madrid JF. CD34+ stromal cells/fibroblasts/fibrocytes/telocytes as a tissue reserve and a principal source of mesenchymal cells. Location, morphology, function and role in pathology. *Histol Histopathol.* 2014;29(7):831–870.
41. Rusu MC, Cretoiu D, Vrapciu AD, Hostiuc S, Dermengiu D, Manoiu VS, Cretoiu SM, Mirancea N. Telocytes of the human adult trigeminal ganglion. *Cell Biol Toxicol.* 2016;32(3):1–9.
42. Mandache E, Popescu LM, Gherghiceanu M. Myocardial interstitial Cajal-like cells (ICLC) and their nanostructural relationships with intercalated discs: shed vesicles as intermediates. *J Cell Mol Med.* 2007;11(5):10.
43. Popescu LM, Gherghiceanu M, Suciuc LC, Manole CG, Hinescu ME. Telocytes and putative stem cells in the lungs: electron microscopy, electron tomography and laser scanning microscopy. *Cell Tissue Res.* 2011;345(3):391–403.
44. Fertig ET, Gherghiceanu M, Popescu LM. Extracellular vesicles release by cardiac telocytes: electron microscopy and electron tomography. *J Cell Mol Med.* 2015;18(10):1938–1943.